NRAO Summer Student Lecture Series
July, 1971
Bruce Balick

INTERFEROMETRY AND APERTURE SYNTHESIS

I. INTRODUCTION

Electromagnetic radiation is a wave phenomena implying instruments used to observe this radiation are subject to diffraction limitations on their resolution. The angular limit, $\Delta\theta$, is given approximately by $\Delta\theta \sim D/\lambda$ where D is the aperture dimension and λ is the observing wavelength; for radio work

$$\frac{\Delta\theta}{\text{min arc}} = 140 \frac{[\lambda/\text{cm}]}{[D/\text{feet}]} .$$

Thus the 300' telescope has a maximum resolution of ~6' arc at λ11 cm, where as a 10 cm aperture optical telescope has a diffraction limit of 1" arc at optical wavelengths. (The same high resolution would require apertures 1-1000 km in diameter at radio wavelengths).

To obtain high resolution resolution at radio wavelengths, partially filled apertures of large diameter can be synthesized. For this, two telescopes separated by a baseline $\underset{\sim}{B}$ can be used to simulate the response of a nearly circular annulus of diameter $|B|$. The telescope pair is configured in such a manner that it is best described as an interferometer in the ordinary optical sense. By moving the telescopes to obtain interferometers of different spacings, annuli of different diameters can be simulated. The results obtained on the various spacings can be added appropriately to synthesize the response of a single telescope of very large diameter, and thereby yield maps of high resolution. For example, the NRAO interferometer can be used to synthesize an aperture of 2.7 km diameter. At a wavelength of 3.7 cm, the resolution is 3" arc.

We shall investigate the response of an ideal interferometer to an ideal source of radiation. As the discussion proceeds, we shall relax some of the restrictions to discuss more realistic sources and instruments. Finally, we shall discuss how a high resolution map is obtained. Complementary discussions can be found in

Tyler, W. C., NRAO Summer Student Lect. Ser., 1966.

Miley, G. K., NRAO Summer Student Lect. Ser., 1969.

McDonald, G. H., NRAO Summer Student Lect. Ser., 1969.

Hogg, D. E., NRAO Internal Reports, June, 1968.

Swenson, G. W., Jr., and Mathur, N. C., 1968, Proc. IEEE, **56**, 2114.

II. RESPONSE OF AN INTERFEROMETER

An ideal interferometer consists of two identical telescopes joined by equal lengths of cable into a multiplier where the noiseless signals from both telescopes are multiplied (correlated). The ideal source is a stationary monochromatic point source at infinity. We shall drop some of these assumptions. The discussion which follows in this section has a close analogy in the case of the optical double slit interferometer.

The ideal interferometer is shown schematically in Figure 1. $\mathbf{B}$ is the vector baseline separation, measured in wavelengths. The specific coordinate system used to describe $\mathbf{B}$ is not important, and will be chosen for convenience later. The output voltages of the RF amplifiers of telescopes 1 and 2 are*

---

* In the discussion which immediately follows, it is assumed (but is not essential) that the reader is familiar with the response of the electronics typically found on single dish telescopes.

$$V_1 = 1/2\ \Delta f\ GE \cos\ (2\pi \frac{c}{\lambda} t)$$
$$= V_{01} \cos\ (2\pi\ ft)$$
$$V_2 = V_{02} \cos\ (2\pi\ ft + \phi)$$

where E is the strength of the incoming signal, G is the amplifier gain, f is the observing frequency, V_{01} and V_{02} are the output voltages (assumed to be equal), and the 1/2 arises because we measure only one polarization. $\phi = 2\pi\ \Delta\ell/\lambda$ is the lag of the signal from telescope 2 arising because the path length from 2 is greater by an amount $\Delta\ell = s|B|\cos\theta$ where s is a unit vector in the direction of the source. The RF signals are mixed by a common local oscillator to obtain the IF signals which are then multiplied in the correlator. The multiplier output M is thus given by

$$M = V_1 V_2 = V_o^2 \cos\ (2\pi\ f_{IF} t) \cos\ (2\pi\ f_{IF} t + \phi)$$
$$= 1/2\ V_o^2\ [\cos\phi + \cos\ \{2\pi(2f_{IF})t + \phi\}].$$

The second term is rejected by the low pass filter whose output R, is thus proportional to $V_o^2 \cos\ (2\pi\ \Delta\ell/\lambda)$. If the source were stationary with respect to the baseline this output would be a constant; however, because the source (as seen from the baseline) appears to move as the earth rotates, $\Delta\ell$ changes by many wavelengths and the output varies nearly sinusoidally resulting in the characteristic "fringe" pattern (each fringe results from a change in $\Delta\ell$ of one wavelength). The amplitude of the fringes is directly proportional to the source strength S, where S is the radio flux density of the source,

$$\boxed{(1)\quad R\ \alpha\ V_o^2 \cos\ [2\pi\ |B| \cos\theta]\ \alpha\ S \cos 2\pi\ \underset{\sim}{B}\cdot\underset{\sim}{s}\ .}$$

This is the first fundamental equation of interferometry. Examples of fringes are shown in Figure 2.

The interferometer response can be alternately pictured as a set of fixed sinusoidal lobes which are parallel, but not quite equally spaced (the spacing is discussed below). The "comb" of lobes are shown in various aspects in figures 3a, 3b, and 3c. Sources move through the comb as the earth rotates. The paths of sources at $\delta = 0°$, $30°$, and $60°$ are shown. Also indicated is the tracking limit of the telescopes at hour angles of $\pm 6^h$.

These lobes are not a property of the individual antennae, but only of their relative placement and their orientation with respect to the instantaneous direction of the source. To repeat, <u>fringes are a result of the changing source, baseline geometry</u>. They are independent of the observing frequency if $\underset{\sim}{B}$ is measured in wavelengths. The primary antennae patterns of the single dish telescopes do not directly enter into the fringe pattern, but merely select a region of the sky over which radiation from sources moving through the lobes can be observed. Thus the individual antennae must track the source.

The lobe separation is the angular separation of adjacent lobe maxima, $\Delta\theta$. $\Delta\theta$ is determined by the condition that $2\pi\,|B|\cos\theta$ changes by 2π. Let θ_1 and θ_2 be two angles for which $|B|\cos\theta$ changes by unity; that is,

$$\theta_2 = \theta_1 + \Delta\theta$$

$$2\pi\,|B|\,(\cos\theta_1 - \cos\theta_2) = 2\pi$$

Substituting and expanding cos $(\theta + \Delta\theta)$ we arrive at

$$|B| \sin \theta \, \Delta\theta = 1 \text{ for } \theta_1 \simeq \theta_2 \simeq \theta.$$

Then

$$\boxed{(2) \qquad \Delta\theta = \frac{1}{|B| \sin \theta} = \frac{1}{|\underset{\sim}{B} \times \underset{\sim}{s}|}}$$

which is the second basic equation of interferometry. $\underset{\sim}{B} \times \underset{\sim}{s}$ is the component of the baseline which is perpendicular to the direction of the source. That is, <u>$\Delta\theta$ is determined by the projected baseline, as seen by the source</u>.

When sources pass through the meridian of the baseline (b_m) the effective baseline, and thus the no. of fringes traversed per unit time, is a maximum. Also, the lobe separation is a minimum. When the source crosses over the end of the baseline (called crossover), the baseline projection goes through a minimum. In addition, the source is moving in a direction which is instantaneously parallel to the lobes so no lobes are traversed, and the fringe rate instantaneously drops to zero. See figures 2 and 3c.

Let us view the baseline from the source in order to define some important new variables. Imagine an observer fixed on the source who sees the baseline change below him as the earth rotates. The baseline, projected onto his sky, ascribes a smooth curve. He can measure an east-west and north-south component of the instantaneous baseline projection; call these u and v. The geometry is shown in figure 4. As the earth rotates, the baseline "turns" and u and v change. For sources nearly overhead, the ends of the baseline ascribe almost circular paths. These paths, for sources at different declinations, are shown in figure 5 for a possible baseline of the NRAO interferometer. The abscissa is u and the ordinate v. The baseline itself is shown in figure 6. Indicated on the figure are the possible telescope positions. Telescope separations of 1, 2, 3, 4, 5, 6, 7, 8, 9, 12, 18, 19, 21, 24, and 27 hundred meters are possible. In figure 7, all the available projected baselines that can be seen by sources of different declinations are visible. Ten divisions on the grid correspond to 25,000λ at λ11.1 cm, and 75,000λ at λ3.7 cm (the observing frequencies of the NRAO instrument).

The graphs of figure 7 indicate all the spacings that a source at one of the declinations can see. This statement means exactly the same as the following:

> The aperture which can be synthesized for the observation of a source at any declination is the sum total of all projected baselines as plotted in the u, v plane.

Thus the elliptical rings of figure 7 are a picture of the partially filled aperture which can be synthesized. It remains to be seen how the fringes observed at those points in the (u, v) plane can be used to construct a high resolution map. For interest, the beam pattern of the synthesized aperture for sources at declinations of 60°, 30°, and 0° are shown in figures 8(a), (b), and (c). In figure 8(d), the effect of neglecting the 600 meter spacing (arbitrarily chosen) on the synthesized beam is shown -- it is negligible.

It should be intuitively recognizable that u and v form a fundamental set of coordinates. Just how fundamental will be shown later. First we pause to establish some convenient coordinate systems so as to express u and v in terms of more intuitively obvious quantities like the hour angle H, the declination δ, and the baseline length $B = |\underset{\sim}{B}|$. We shall also derive the equations for the elliptical annuli of figure 7.

We define a rectangular coordinate system which has components (x, y, and z) along perpendicular directions in the equatorial plane and the north pole. These directions are fixed with respect to the ground.* The basic geometry of the (x, y, z) coordinate system is depicted in figure 4. The source, located in the direction of the vector $\underset{\sim}{s}$ has (changing) hour angle H and declination δ as shown in the figure. The baseline $\underset{\sim}{B}$ would appear as a fixed line passing through the origin (but not necessarily in the (x, y), or equatorial plane). The baseline could be defined by its length B and two fixed direction angles called the baseline hour angle h and declination d. Then

$$\begin{pmatrix} B_x \\ B_y \\ B_z \end{pmatrix} = \begin{pmatrix} B \cos d \cos h \\ B \cos d \sin h \\ B \sin d \end{pmatrix} \quad \text{and} \quad \begin{pmatrix} s_x \\ s_y \\ s_z \end{pmatrix} = \begin{pmatrix} \cos \delta \cos H \\ \cos \delta \sin H \\ \sin H \end{pmatrix}$$

---

* That is, if ψ is the latitude of the observing site, then the baseline $\underset{\sim}{B}$ on the ground has projections

$$\begin{pmatrix} B_x \\ B_y \\ B_z \end{pmatrix} = \begin{pmatrix} -\sin \psi & 0 & \cos \psi \\ 0 & -1 & 0 \\ \cos \psi & 0 & \sin \psi \end{pmatrix} \begin{pmatrix} B_{north} \\ B_{east} \\ B_{zenith} \end{pmatrix}$$

where B_{zenith} is 0 for baseline on level ground.

and $\cos\theta = \underset{\sim}{B}\cdot\underset{\sim}{s}/B = \sin d \sin\delta + \cos d \cos\delta \cos(H-h)$. The projected baseline $\underset{\sim}{B} \times \underset{\sim}{S}$ changes with hour angle, but can at any time be resolved into its u, v components as shown in the figure. By inspection

$$\begin{pmatrix} u \\ v \\ B \end{pmatrix} = \begin{pmatrix} \sin H & -\cos H & 0 \\ -\sin\delta\cos H & -\sin\delta\sin H & \cos\delta \\ \cos\delta\cos H & \cos\delta\sin H & \sin\delta \end{pmatrix} \begin{pmatrix} B_x \\ B_y \\ B_z \end{pmatrix} .$$

These matrix representations of the geometry were developed by Dr. C. M. Wade.

It can easily be verified that

$$\frac{u^2}{a^2} + \frac{(v - v_o)^2}{b^2} = 1$$

where $a = \sqrt{B_x^2 + B_y^2} = B\cos d$, $b = a\sin\delta = B\cos d\sin\delta$, and $v_o = B_z\cos\delta = B\sin d\cos\delta$. This is the equation of an ellipse centered at ($u = 0$, $v = -B\sin d\cos\delta$) with major axis a, minor axis b, and eccentricity $\cos\delta$. Note that only the minor axis and ellipse center depend on the source position.

The minimum lobe separations (i.e., those available at the instrumental meridian where the effective baseline is the true baseline) are shown in table 1.

Baseline (100 meters)	1	2	3	4	5	6	7	8
Lobe separation	3!8	1!9	1!3	57"	46"	38"	33"	28"

Baseline (100 meters)	9	12	15	18	19	21	24	27
Lobe separation	25"	19"	15"	13"	12"	11"	10"	8".5

III. RESPONSE TO EXTENDED SOURCES

It is the purpose of this section to establish the relationship between the observed fringe pattern and the source brightness distribution, and to describe how the high resolution map is obtained. We must first define those parameters that describe the observed fringe pattern and show, in a semi-intuitive fashion, how they relate to the source geometry. The precise relation between the source structure and interferometer response will then be developed.

The low pass filter output R (i.e., the fringe pattern) can be written as

(3) $R = A \cos (2\pi \underset{\sim}{B} \cdot \underset{\sim}{s} + \Phi)$

where A is called the fringe amplitude (or colloqiually the amplitude), Φ is the fringe phase, or phase, and $2\pi \underset{\sim}{B} \cdot \underset{\sim}{s}$ is the fringe period which is entirely a property of the source - earth geometry and has nothing to do with source structure. As a matter of procedure, the amplitude and phase are computed by an on-line computer (every 30 sec in the case of the NRAO interferometer) by a least squares fit to a sine wave of the expected period. The amplitude is the height of the fringes, and the phase is defined as the shift of the measured fringes with respect to the fringe pattern that would result from an ideal point source at the same position in the sky. We now discuss the meaning of the amplitude and phase in more detail.

The amplitude, as we have established, is proportional to the flux of a point source. This, however, is not the case for an extended source. Consider now an extended source, say one of uniform brightness, that is sufficiently large that it spans more than one lobe, say N lobes.

As the source moves through the lobes, it occupies all except perhaps one of them at any time. Compare this to a point source of the same flux S which would occupy either zero or one lobe. If the energy output of the low pass filter for the point source is proportional to S for the point source, then it would be of order $S \times [N-(N-1)]/N = S/N$ for the uniform extended source. In general, the larger the ratio of source size to lobe separation, the smaller the observed amplitudes for sources of the same flux.

Say many parallel pairs of telescopes of different separations simultaneously observe the same source. It follows that the amplitudes observed on the smaller spacings will be larger than those of the outer spacings for a source which is sufficiently extended. If the response to a source is found to fall off at a certain spacing, the source is said to be "resolved" at that spacing; otherwise it is unresolved. A plot of amplitude vs. spacing is called the real visibility function (this, we shall see, is a slight misnomer). Variations in this function are related to source structure; however, the real visibility function is not sufficient information from which to unambiguously derive a map of the source. The fringe phases clear up any ambiguities.

The meaning of the fringe phase is somewhat more esoteric. The phase is related to the apparent instantaneous brightness centroid offset from the center of the field of view; i.e., it is sensitive to position (this description of the phases has severe limitations). Consider a point source whose position is well known (to a small fraction of the lobe separation). Its fringe pattern has zero phase. Now displace the source a fraction of a lobe separation. The measured fringe pattern will have the same period (actually $\underset{\sim}{s}$ changes slightly but differences in the period can generally be ignored) but the fringes will not arrive at the expected time. If the source is displaced by half a lobe, the fringe phase will be 180°. If the source is displaced by an angular distance $\Delta\phi$ and the lobe separation is $\Delta\theta$, the phase (in radians) will be $2\pi\ \Delta\phi/\Delta\theta$. Here it was assumed that the displacement of the source was along a line perpendicular to the lobes.

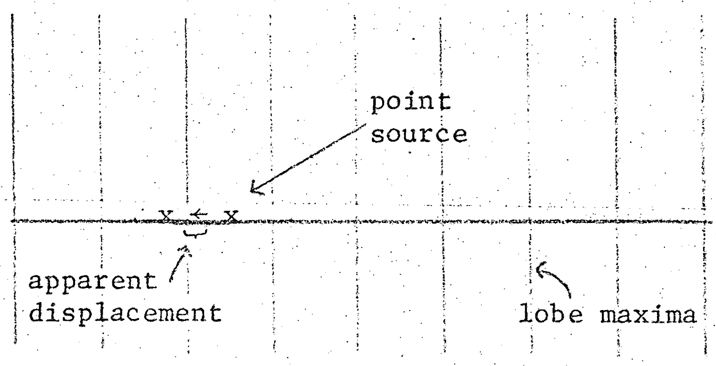

Displacement of a point source in the discussion above.

As the source moves through the sky, it sees the baseline orientation, and thus the lobe orientation rotate slowly. Then the displacement of the displaced point source, projected onto a line perpendicular to the lobes, also changes; the phases change accordingly.

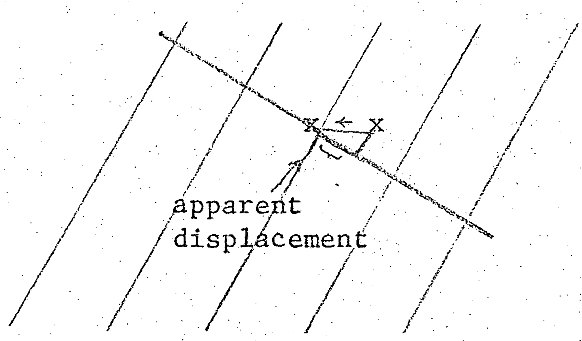

Displacement of the point source above at a different time.

Then the response R is given by A cos $\{2\pi\ \underset{\sim}{B}\cdot(\underset{\sim}{s} + \Delta \underset{\sim}{s})\}$, or $\Phi = 2\pi\ \underset{\sim}{B}\cdot\Delta\underset{\sim}{s}$, where $\Delta\underset{\sim}{s}$ is the source displacement. Letting the displacement have E-W component $\Delta\alpha \cos \delta$ and N-S component $\Delta\delta$, and recalling the difinition of u and v we obtain

$$\begin{aligned}\Phi\ (H,\ \delta) &= u\cdot\Delta\alpha \cos \delta + v\cdot\Delta\delta \\ &= \Delta\alpha\ (B_x \cos \delta \sin H + B_y \cos \delta \cos H) \\ &\quad + \Delta\delta\ (-B_x \sin \delta \cos H + B_y \sin \delta \sin H + B_z \cos \delta)\end{aligned}$$

Note this implies that the phases can be represented as a flat plane which intersects the (u, v) plane along the line $u\cdot\Delta\alpha \cos \delta + v\cdot\Delta\delta = 0$. The phase behavior as the (u, v) ellipse is tracked is easily understood.

An identical discussion pertains to the phase of an extended source with symmetry such that its brightness centroid always appears stationary. This includes sources with circular symmetry and double sources (if the amplitudes are allowed to be negative - see below). For very irregular sources the apparent brightness centroid changes erratically with a corresponding irregular phase behavior. See figure 10.

Having laid an intrutive groundwork for understanding the fringe amplitude and phase we now show that both uniquely define a map, and in addition we show how to construct the map. Consider an extended source contained well within the primary antennae beams. Let its brightness distribution be $T(\alpha, \delta)$. Let α_o and δ_o denote a reference position near the source - say the center of the primary beam. We can define cartesian coordinates (x, y) in the plane of the sky with origin at (α_o, δ_o) with $x = (\alpha-\alpha_o) \cos \delta$ and $y = (\delta-\delta_o)$; then x and y are not scaled by cos δ as α and δ are. An infinitesimal area in the source has intensity $T(x, y)\,dxdy$. The interferometer response to this element alone is identical to that of a point source:

$$dR \propto T(x, y) \cos (2\pi\, B \cos \theta) dxdy.$$

As stated previously, we may assume that the source dimensions, are small so that the period of the fringes are the same over the entire source. This allows us to write the argument of the cosine in the form of equation (3):

$$dR \propto T(x, y) \cos \{2\pi\, B \cos \theta + 2\pi\, (ux+vy)\}$$

where the phase $\Phi = 2\pi\, \underset{\sim}{B} \cdot \Delta \underset{\sim}{s} = 2\pi(ux+vy)$. The same equation can be derived by a Taylor expansion of $\cos \theta$ about the origin. For simplicity let us define $\Phi_o = 2\pi\, B \cos \theta$. Then expanding the cosine of a compound angle we obtain,

$$dR(u, v) \propto T(x, y)\, dx\, dy\, \{\cos [2\pi(ux+vy)] \cos \Phi_o - \sin [2\pi(ux+vy)] \sin \Phi_o\}$$

Integrating over the source, we obtain the total response,

$$(4) \quad R(u, v) \propto S\, \{\underset{\sim}{R}(u, v) \cos \Phi_o - \underset{\sim}{I}(u, v) \sin \Phi_o\}$$

where $\underset{\sim}{R}$ and $\underset{\sim}{I}$ are the normalized cosine and sine Foruier transforms of the source brightness distribution

$$\begin{Bmatrix} \underset{\sim}{R} \\ \underset{\sim}{I} \end{Bmatrix} = \frac{1}{S} \frac{2k}{\lambda^2} \int_{-\infty}^{\infty}\int_{-\infty}^{\infty} T(x, y) \begin{Bmatrix} \cos \\ \sin \end{Bmatrix} [2\pi(ux + vy)]\, dx\, dy$$

Here S is the usual flux density given by $\frac{2k}{\lambda^2} \iint_{-\infty}^{\infty} T(x, y)\, dx\, dy$. Note that for a point source $\underset{\sim}{R} = 1$ and $\underset{\sim}{I} = 0$ resulting in equation (1).

Because $T(x, y)$ is a real function, so are $\underset{\sim}{R}$ and $\underset{\sim}{I}$. We can therefore define the complex visibility function $\underset{\sim}{V}(u, v) \equiv \underset{\sim}{R}(u, v) + i\underset{\sim}{I}(u, v)$, where R and I are its real and imaginary components. We can alternatively express $\underset{\sim}{V}$ in terms of an amplitude and phase,

$$(5) \quad \underset{\sim}{V}(u, v) \equiv A(u, v)\, e^{i\Phi(u, v)}$$

It follows that

$$A(u, v) = \{\underset{\sim}{R}^2(u, v) + \underset{\sim}{I}^2(u, v)\},$$

$$\text{and } \Phi\ (u, v) = \tan^{-1}\left(\frac{\underset{\sim}{R}(u, v)}{\underset{\sim}{I}(u, v)}\right)^{-1}.$$

We can formally substitute these relations into equation (4):

$$R\ \alpha\ \{\underset{\sim}{R}^2 + \underset{\sim}{I}^2\}^{1/2}\left[\frac{\underset{\sim}{R}}{\{\underset{\sim}{R}^2+\underset{\sim}{I}^2\}^{1/2}}\cos\Phi_o - \frac{\underset{\sim}{I}}{\{\underset{\sim}{R}^2+\underset{\sim}{I}^2\}^{1/2}}\sin\Phi_o\right]$$

$$= A(u, v)\ \{\cos\Phi\cos\Phi_o - \sin\Phi\sin\Phi_o\}, \text{ or}$$

$$(6) \quad \boxed{R\ \alpha\ A(u, v)\cos\{2\pi\ \underset{\sim}{B}\cdot\underset{\sim}{s} + \Phi(u, v)\}}$$

which is identical to equation (3). Then the mathematically defined functions A and Φ take on a physical significance as the fringe amplitude and phase. That is, the fringe amplitude and phase are the amplitude and phase of the complex visibility function $\underset{\sim}{V}(u, v)$, which itself is built from the Fourier sine and cosine transform of the brightness distribution. A much clearer interpretation results from some last algebraic manipulation; from the definition of $\underset{\sim}{V}$, $\underset{\sim}{R}$, and $\underset{\sim}{I}$ we have,

$$\underset{\sim}{V} = \underset{\sim}{R}+i\underset{\sim}{I} = \frac{1}{S}\int_{-\infty}^{\infty}\int_{-\infty}^{\infty} T(x, y)\ \{\cos 2\pi\ (ux+vy) + i\sin 2\pi\ (ux+vy)\}\ dx\ dy,$$

or

$$\text{(7)} \quad \boxed{\underset{\sim}{V}(u, v) = \frac{1}{S} \int_{-\infty}^{\infty} \int_{-\infty}^{\infty} T(x, y)\, e^{2\pi i(ux+vy)}\, dx\, dy.}$$

Then from the theory of the Fourier Transform we may write

> THE MEASURED QUANTITIES OF THE INTERFEROMETER, THE FRINGE AMPLITUDE AND PHASE, FORM A COMPLEX FUNCTION $\underset{\sim}{V}(u, v) = A(u, v) \exp(i\Phi(u, v))$ WHOSE FOURIER TRANSFORM IS THE BRIGHTNESS DISTRIBUTION.

The interferometer, then, responds to Fourier components of the brightness distribution which have angular period equal to the lobe separation, and whose structure is oriented along a line perpendicular to the lobes. This is the fundamental equation of aperture synthesis. The source structure to which the interferometer responds is clearly defined, and we have shown that the brightness distribution can be constructed from the fringe amplitude and phase. The fundamental importance of u and v is also clear.

From equation (7) we derive several corallaries which are important. Using the fact that T(x, y) is real and Fourier Transform theory we derive the following:

$$\begin{aligned}
T(x, y) &= S \iint_{\infty}^{\infty} \underset{\sim}{V}(u, v) \exp\{2\pi i\,(ux+vy)\}\, dudv \\
&= S \iint_{\infty}^{\infty} \{\underset{\sim}{R}(u,v) \cos 2\pi\,(ux+vy) + \underset{\sim}{I}(u, v) \sin 2\pi(ux+vy)\} dudv \\
&\quad - iS \iint_{\infty}^{\infty} \{\underset{\sim}{R}(u, v) \sin 2\pi(ux+vy) - \underset{\sim}{I}(u. v) \cos 2\pi\,(ux+vy)\} dudv \\
&\Rightarrow \iint_{\infty}^{\infty} \{\underset{\sim}{R}(u, v) - \underset{\sim}{R}(-u, -v)\} \sin 2\pi\,(ux+vy)\, dudv \\
&\qquad - \iint_{\infty}^{\infty} \{\underset{\sim}{I}(u, v) + \underset{\sim}{I}(-u, -v)\} \cos 2\pi\,(ux+vy)\, dudv \\
&\qquad = 0
\end{aligned}$$

where we have used the parity of the trigonometric functions and the fact that the imaginary part of T(x, y) is 0. Then

$$\underset{\sim}{R}(u, v) = \underset{\sim}{R}(-u, -v) \text{ and } \underset{\sim}{I}(u, v) = -\underset{\sim}{I}(-u, -v), \text{ or}$$

$$\underset{\sim}{V}(u, v) = \underset{\sim}{V}^* (-u, -v)$$

where * denotes comples conjugation. Thus the complex visibility function is said to be "Hermitian". It follows that A(u, v) = A(-u, -v) and $\Phi(u, v) = -\Phi(-u, -v)$, i.e., the amplitudes and phases are redundant on the (u, v) plane. Thus observations need only be taken over half the (u, v) plane. This is why the ellipses in figure 7 have counterparts on the opposite side of the origin.

Secondly, we note that $S \cdot \underset{\sim}{V}(o, o) = \int T(x, y)\, dxdy = S$. That is, the total flux of the source (which is assumed to be contained within the beam) is given by the zero spacing flux at which all sources are unresolved. However, the interferometer cannot measure anything at zero spacing since one telescope would be observing the rear of the second, and not the source. Thus the interferometer cannot be used to measure the total flux of a source unless the source is unresolved at some longer spacing. The failure to sample this point also means that the integral of the brightness temperature over any map must be 0; that is, the average brightness is zero and any sources observed in the map force the remainder of the map to have negative temperatures. This means that negative sidelobes can appear on the map.

An illustrative analogy to the partially filled aperture synthesis technique can be made. Consider a camera mounted in the far field of a grating made of elliptical slits (in the same pattern as the (u, v) ellipses). Consider also a special type of film that is insensitive to the average light intensity level and responds only to differences in light intensity across the subject. The camera and its film would be an instrument which responds in the same manner as the partially filled aperture described in this section.

IV. RESPONSE OF THE NRAO INTERFEROMETER

One picture is worth 1000 words. In Figure 9 the response of the NRAO interferometer at λ11.1 cm has been calculated for symmetric Gaussian sources. (The response at other frequencies scales as the ratio of observing wavelength to 11.1 cm.) For this, the ellipses were assumed to be circular so that a one dimensional analysis was possible. The sources had half power widths (HPW's) as indicated; the beam can be considered a Gaussian of zero width. ξ is the ratio of the peak antenna response to the model sources divided by the peak response to a point source of the same flux. It can be seen that if small and extended sources of comparable flux exist in the same region, then the extended source could be rendered unobservable by the side lobes of greater brightness associated with the small source. This is an important effect which must be rembered when considering aperture synthesis maps.

The beam width of the NRAO interferometer at λ11.1 cm is approximately 8" at half power points in its narrowest dimension. At 40°, the eccentricity of the beam is ~2/3, at 20° it is approximately 1/2, and at 5° it is nearly 1/4. At southern declinations, the inability to track the source for twelve hours generally means the synthesized beam will have eccentricity <0.5, and its narrowest dimension may exceed 8" south of $\delta \sim -20°$.

V. OTHER ASPECTS OF INTERFEROMETRY AND APERTURE SYNTHESIS

We have not considered the following in our discussion:

1) non-identical apertures
2) delay systems necessitated by non monochromatic sources
3) single vs. double side band systems
4) sources larger than the primary antennae beams
5) non-incoherent radiation
6) spectral line and polarization observations
7) calibration problems
8) sources of random, pseudo random, and systematic noise
9) calibration of maps
10) model fitting in the (u, v) plane.

The first 5 of these points, when considered properly, introduce no fundamental changes in the equations presented in this paper. That is not to say these problems can be ignored. Interferometry has been made feasible only because these problems or complications have been overcome, often at great expense. Spectral interferometry is conceptually similar to continuum interferometry. Calibration and noise problems are extremely important and restrict the utility of the interferometer under certain conditions. A general discussion of noise problems will soon be available (Balick, in preparation). The interpretation of the maps, and problems of model fitting will also be discussed.

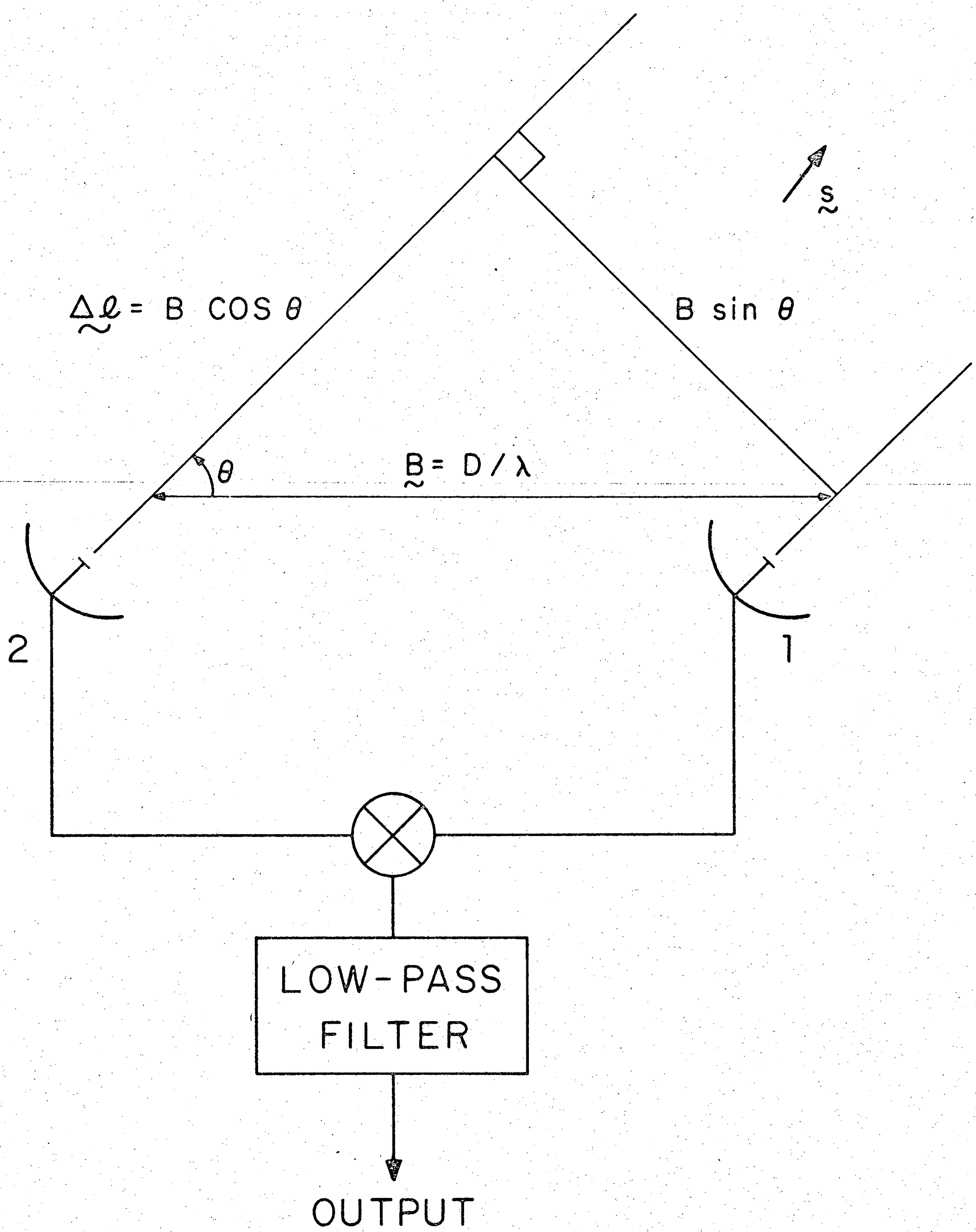

Figure 1. The Idealized Interferometer.

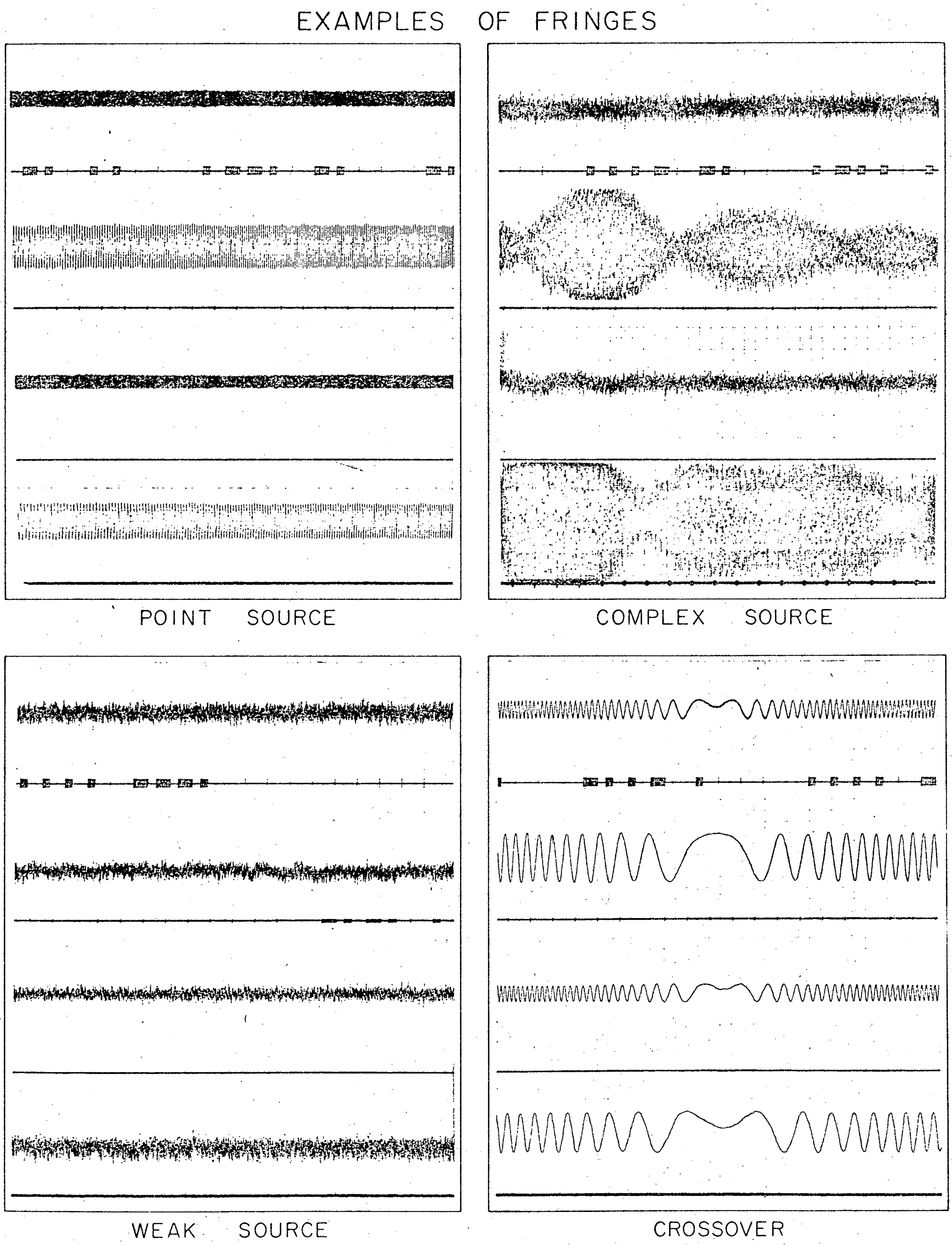

Figure 2. Examples of Fringes.

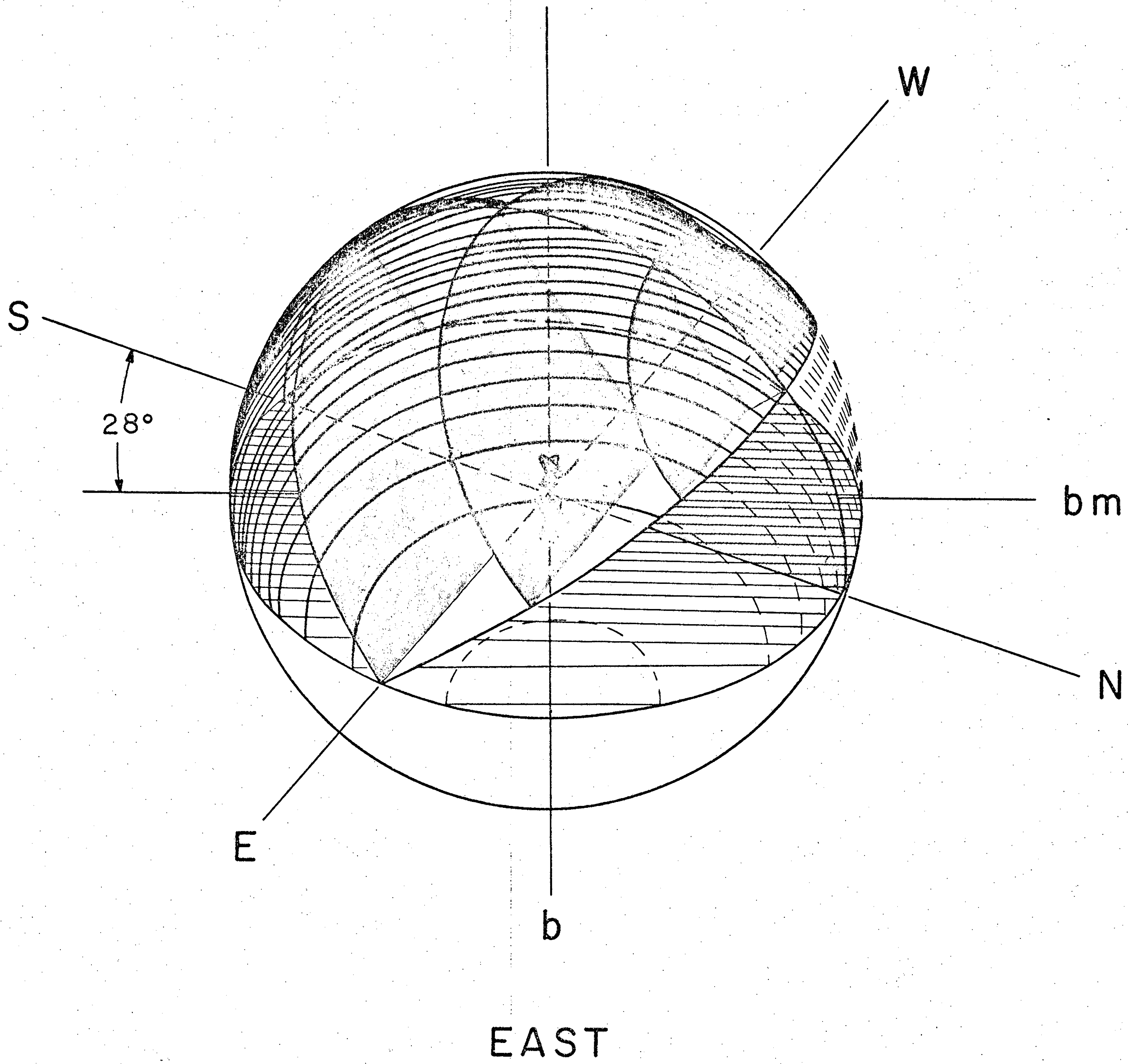

Figure 3a. Lobe-source geometry viewed from the NE end of the baseline. The paths of sources at declinations of 0°, 30°, and 60° are indicated.

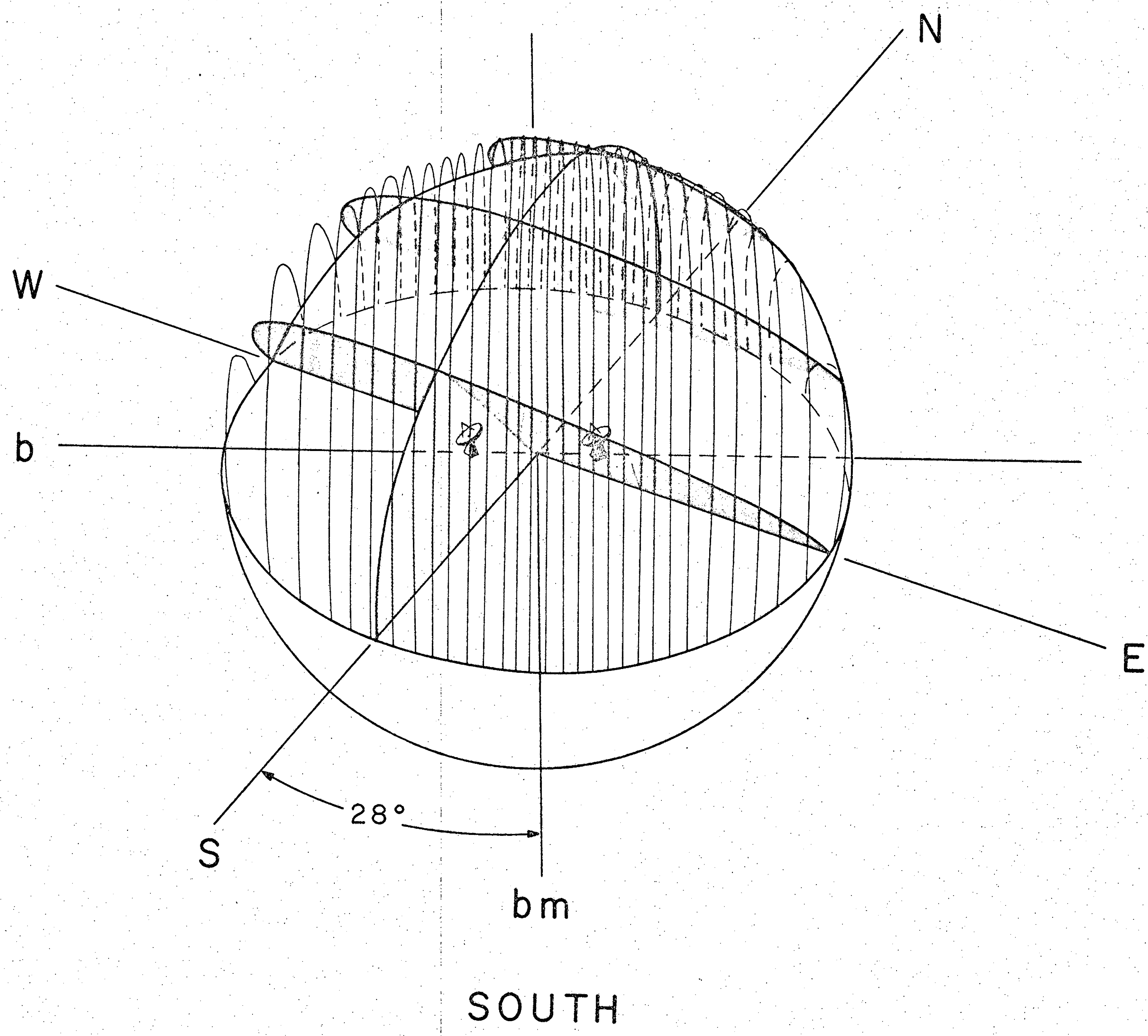

Figure 3b. Lobe-source geometry viewed from the baseline meridian.

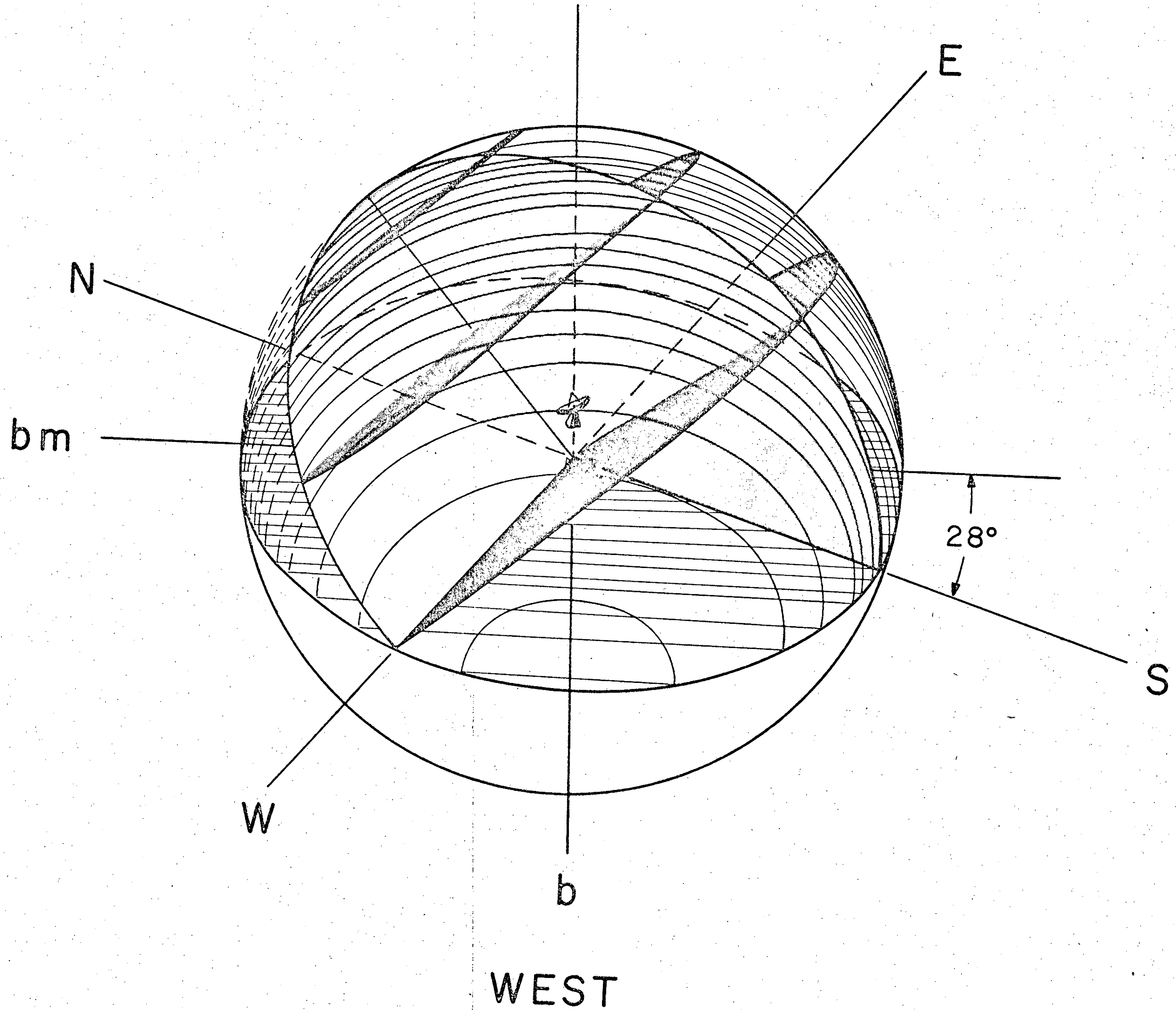

Figure 3c. Lobe-source geometry viewed from the SW end of the baseline.

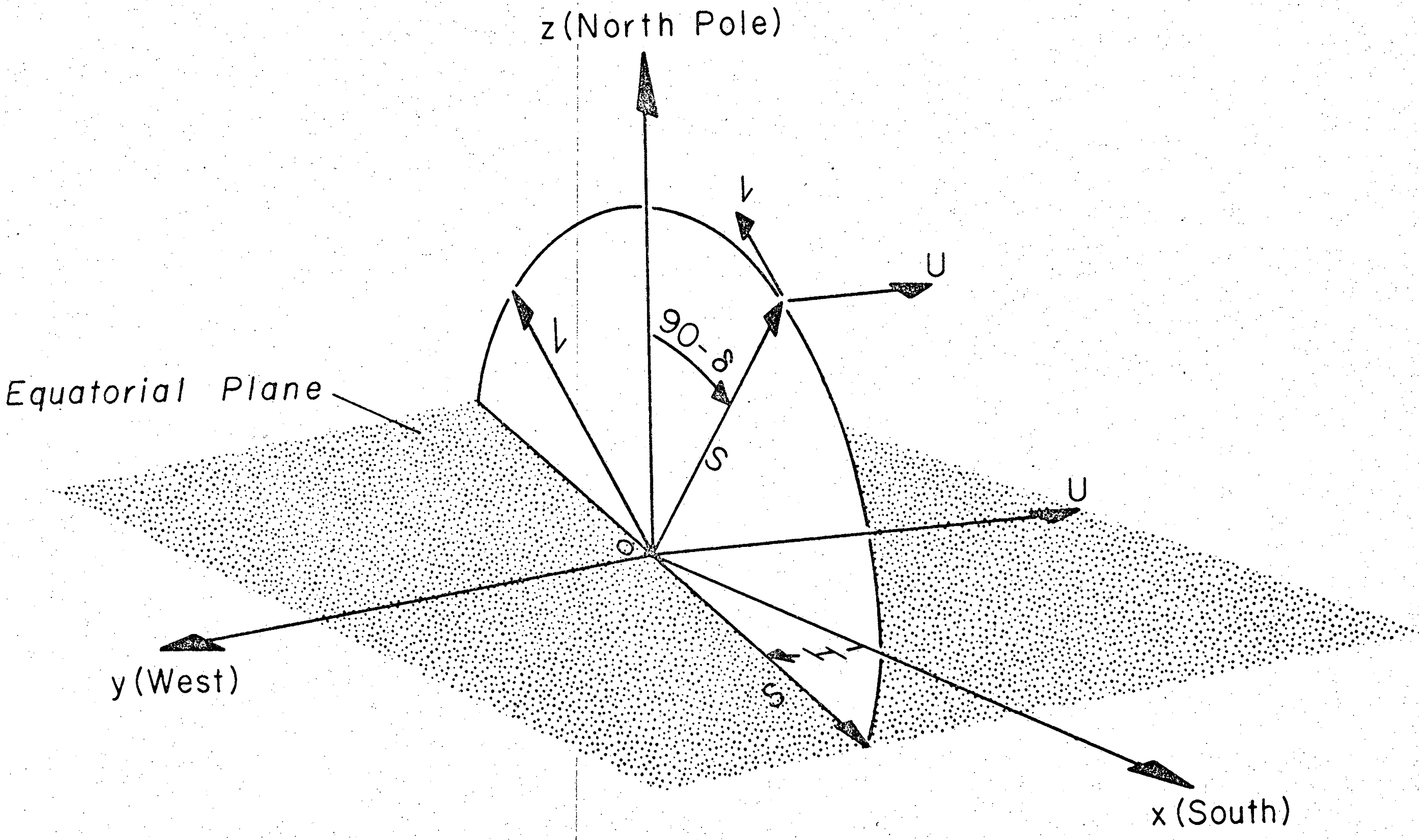

Figure 4. Definitions of the (x,y,z) and (u,v) coordinate systems. The ground plane (not shown) intersects the equitorial plane along the y axis.

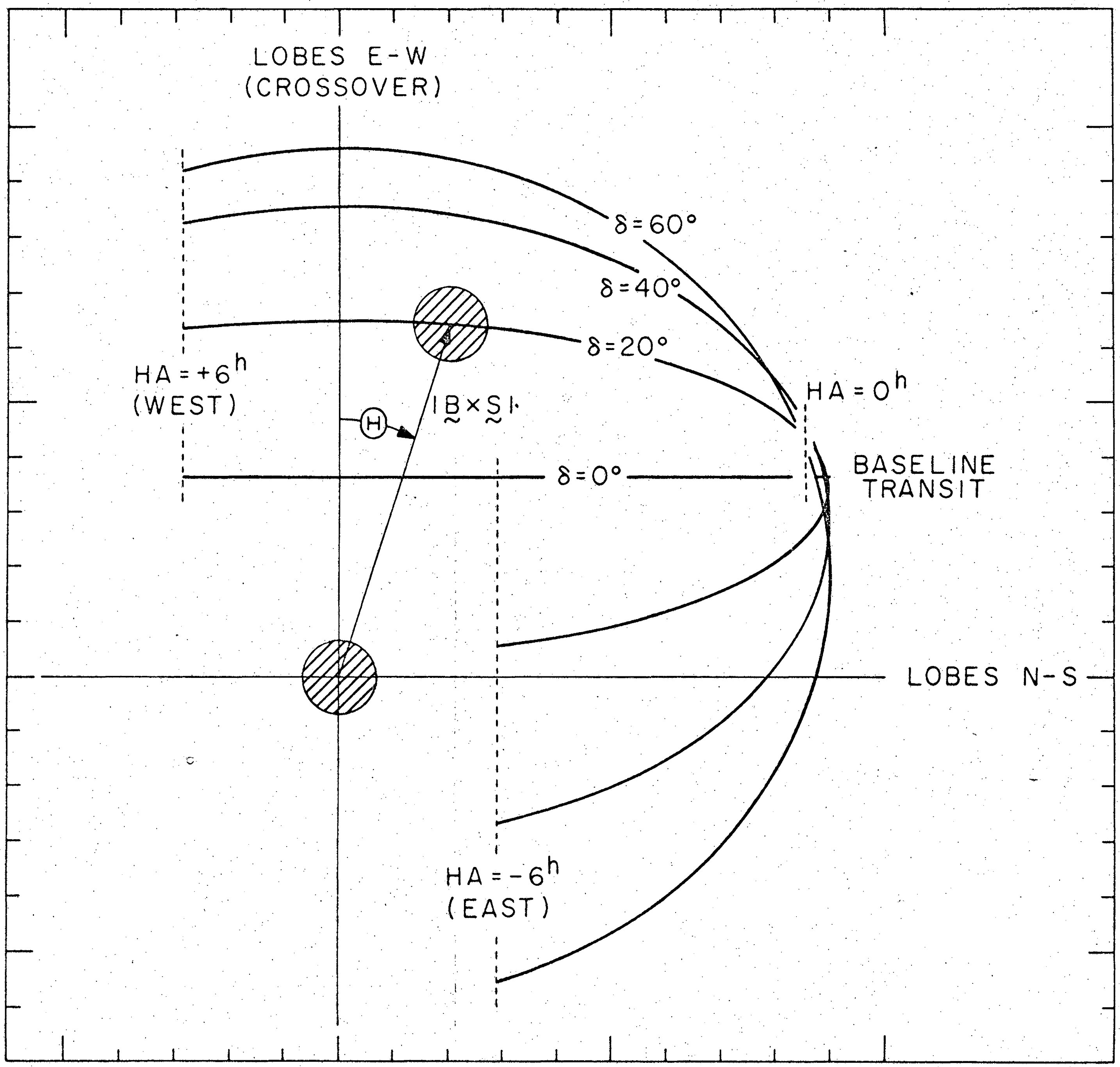

Figure 5. The loci of projected baselines seen by sources at the indicated declinations as they move across the sky.

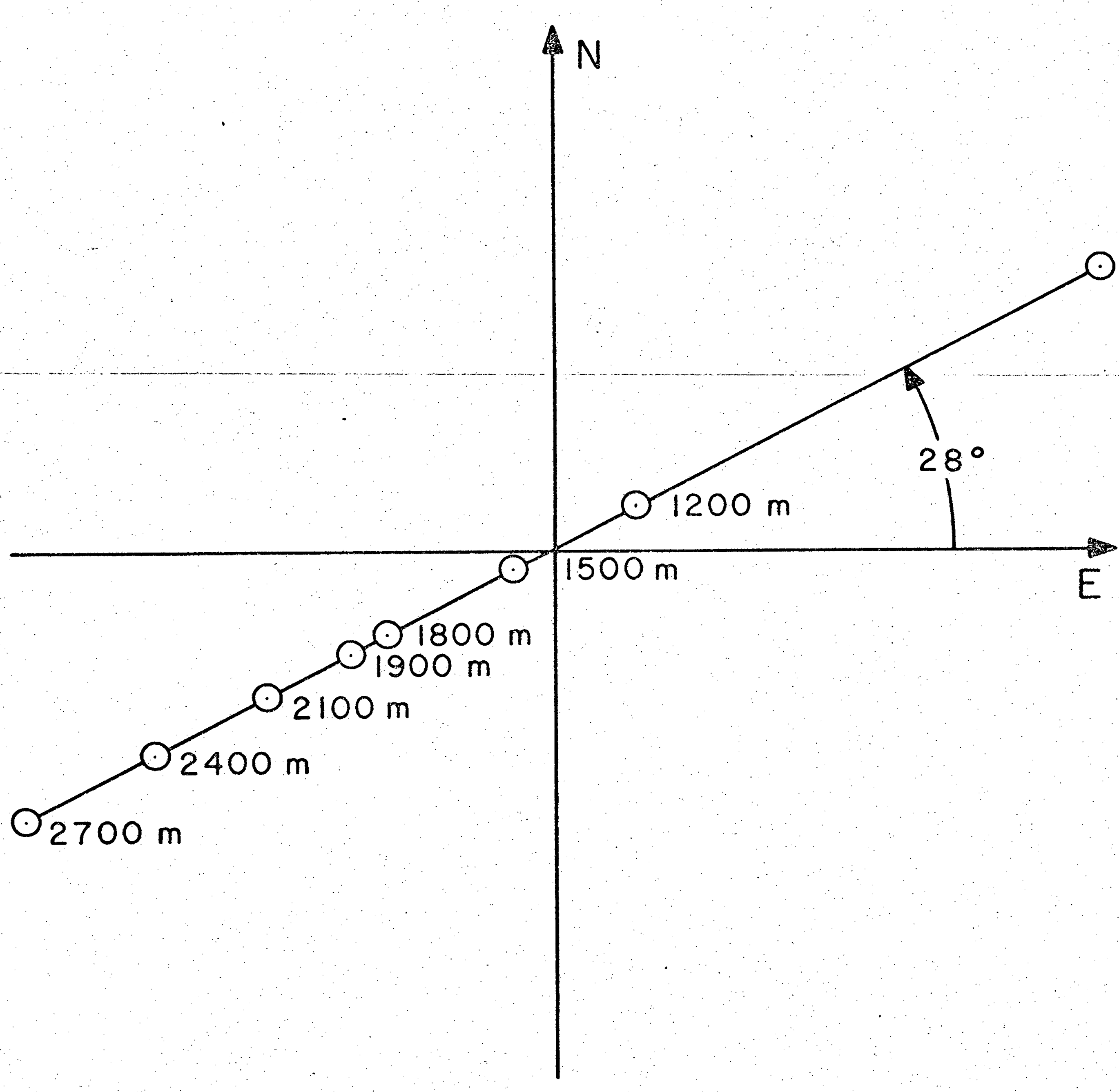

Figure 6. The baseline and available telescope stations for the NRAO interferometer.

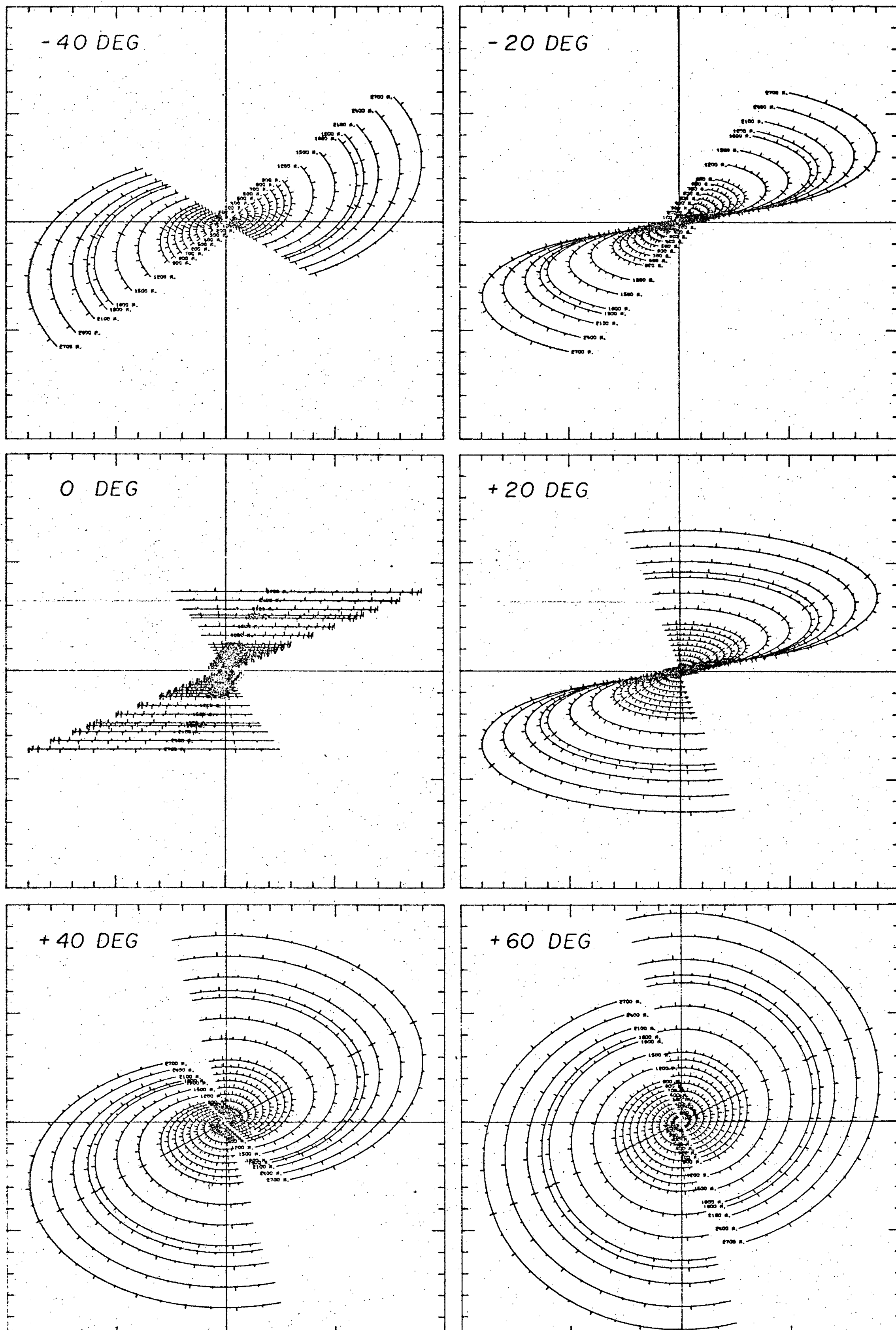

Figure 7. The available baseline coverage, i.e. the synthesized aperture, for sources at the declinations indicated (for the NRAO interferometer). The distance between tic marks is 2500 wavelengths at λ11.1 cm (2695 MHz).

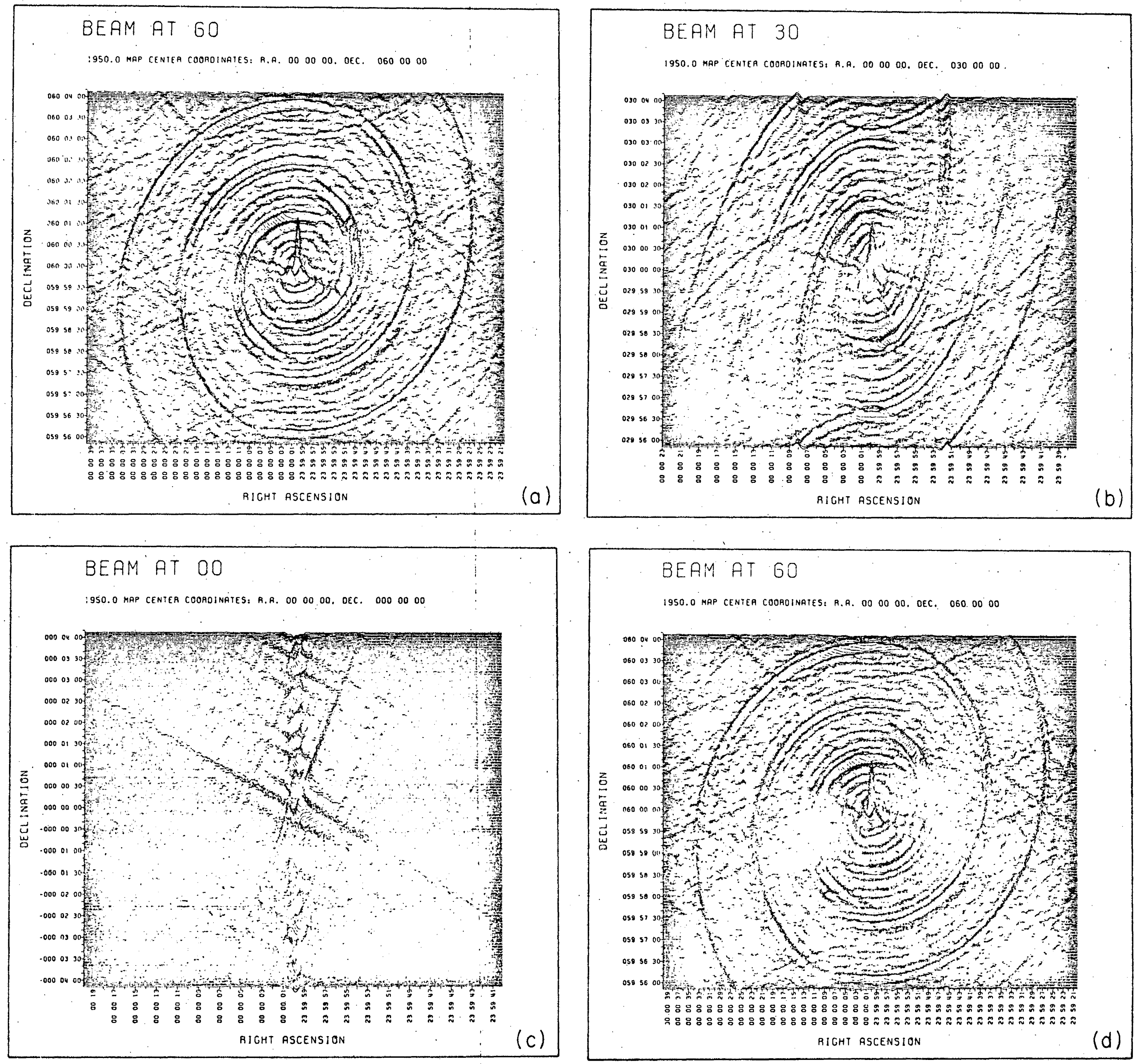

Figure 8. The synthesized beams at = 0 , 30 , and 60 . The baseline coverage used for (d) was that of (a) except that the 600 m spacing was arbitrarily dropped.

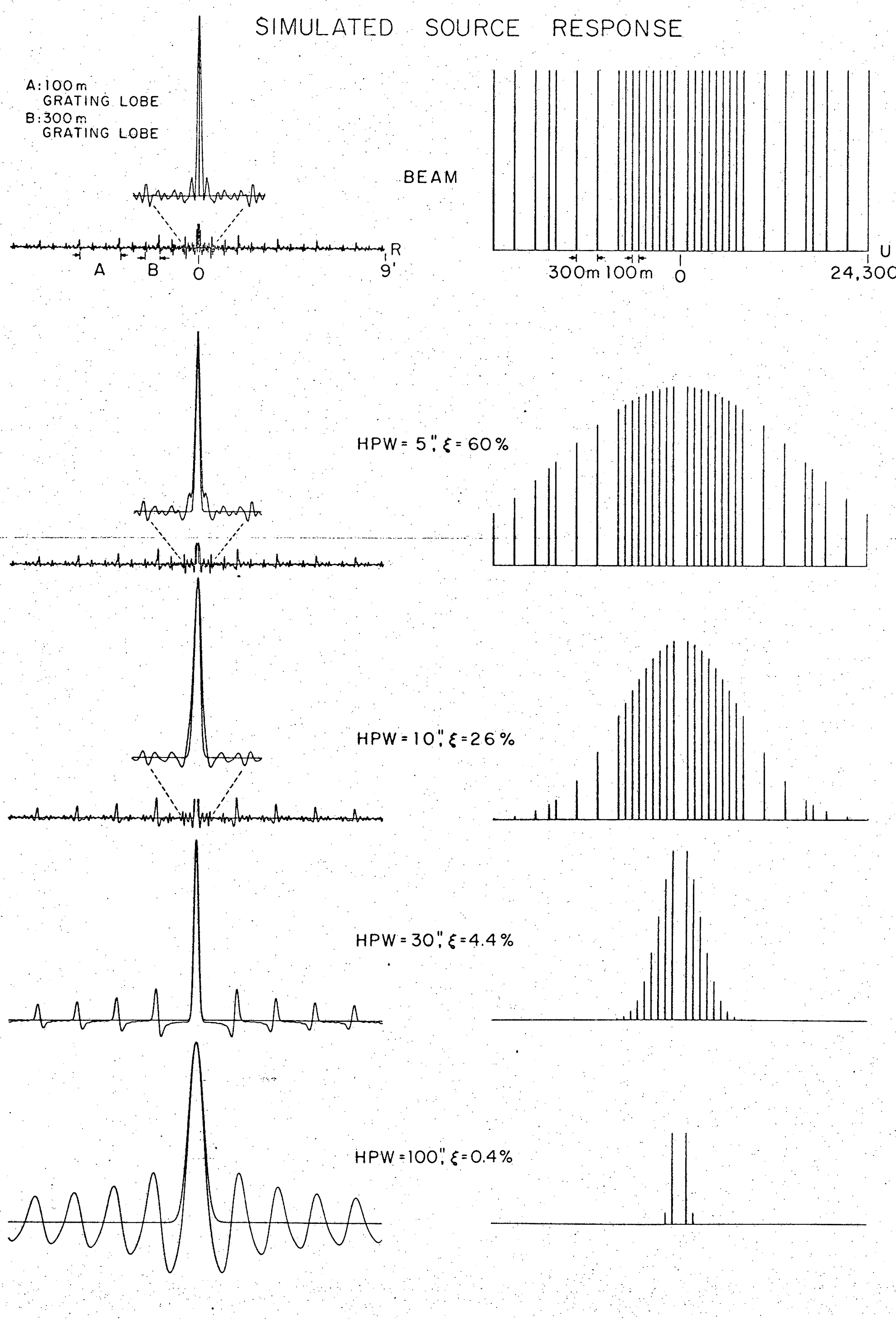

Figure 9. The interferometer response to Gaussian sources of the widths (HPW) indicated. The true, as well as the observed brightness distribution is shown. ξ is explained in the text.

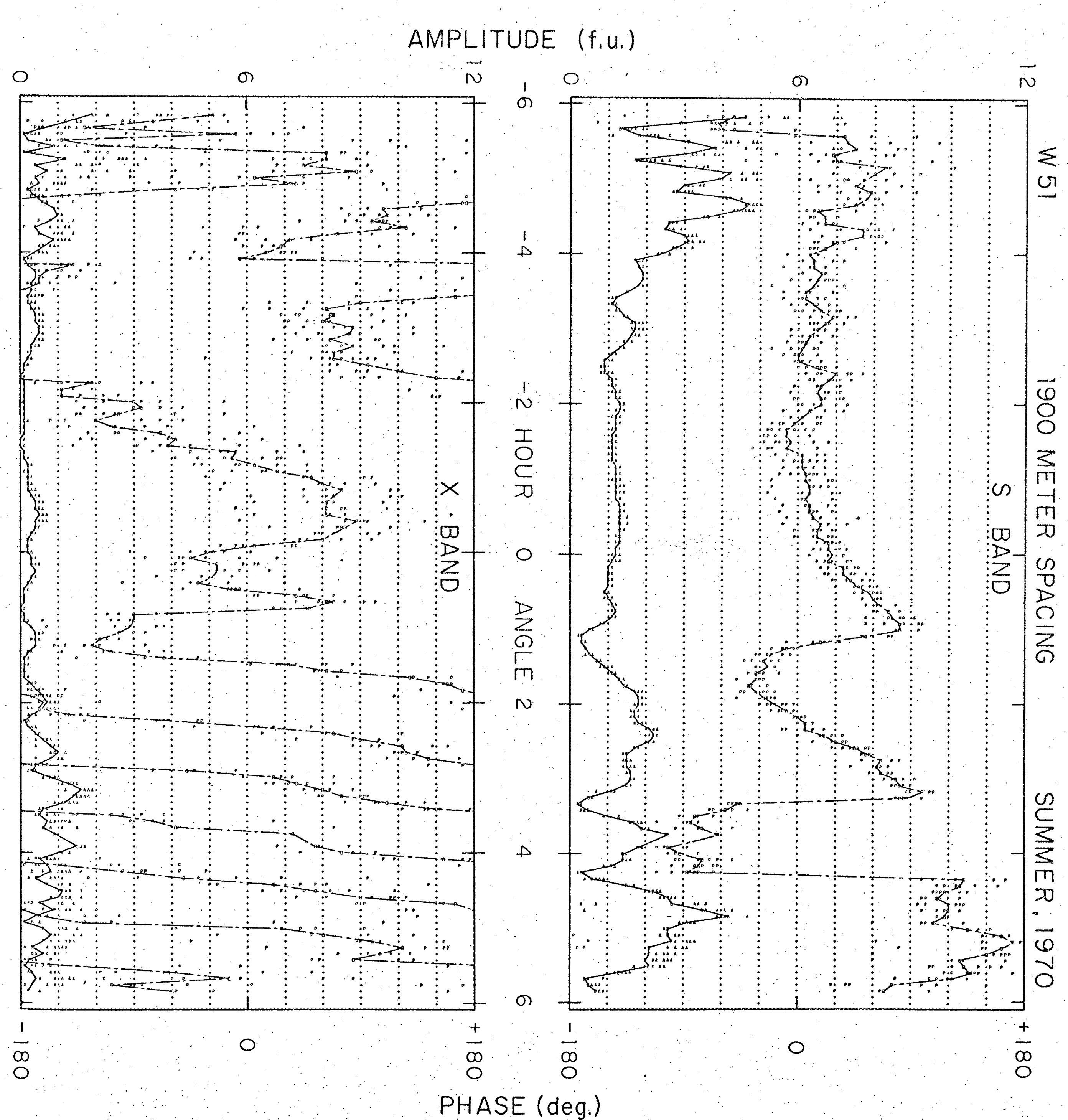

Figure 10. Response of an interferometer to a complex source. Six independent observations are shown. Individual values of the amplitudes and phases ("A" & "P") as well as their vector averages (solid and broken lines) are indicated. S band is λ11.1 cm (2695 MHz); X band is λ3.7 cm.